

University of Wollongong

Research Online

Faculty of Engineering and Information
Sciences - Papers: Part B

Faculty of Engineering and Information
Sciences

2019

Comprehensive Analysis of the Effect of Ausforming on the Martensite Start Temperature in a Fe-C-Mn-Si Medium-Carbon High-Strength Bainite Steel

Junyu Tian

Wuhan University of Science and Technology

Guanghai Chen

Wuhan University of Science and Technology

Yaowen Xu

Wuhan University of Science and Technology

Zhengyi Jiang

University of Wollongong, jiang@uow.edu.au

Guang Xu

Wuhan University of Science and Technology

Follow this and additional works at: <https://ro.uow.edu.au/eispapers1>



Part of the [Engineering Commons](#), and the [Science and Technology Studies Commons](#)

Recommended Citation

Tian, Junyu; Chen, Guanghai; Xu, Yaowen; Jiang, Zhengyi; and Xu, Guang, "Comprehensive Analysis of the Effect of Ausforming on the Martensite Start Temperature in a Fe-C-Mn-Si Medium-Carbon High-Strength Bainite Steel" (2019). *Faculty of Engineering and Information Sciences - Papers: Part B*. 3131.

<https://ro.uow.edu.au/eispapers1/3131>

Research Online is the open access institutional repository for the University of Wollongong. For further information contact the UOW Library: research-pubs@uow.edu.au

Comprehensive Analysis of the Effect of Ausforming on the Martensite Start Temperature in a Fe-C-Mn-Si Medium-Carbon High-Strength Bainite Steel

Abstract

The comprehensive effect of strain and ausforming temperature on the martensite start temperature (M_S) of a medium-carbon bainite steel was investigated by thermal simulation, optical microscope, scanning electron microscope, etc. It is already known that small strain increases the M_S , while larger strain decreases the M_S . However, the effect of ausforming temperature on the M_S has not been reported and clarified. In this study, the concepts of critical strain (ϵ_c) and saturated strain (ϵ_s) are proposed. The M_S at the critical strain is equal to the M_S of the nondeformed specimen. The saturation strain, which is first observed, is the strain value, and the M_S does not further decrease with the increasing strain. The results show that the M_S depends on the strain amount of ausforming but is not affected by the ausforming temperature. Moreover, with the increase of strain amount and ausforming temperature, the length of the martensite laths decreases. In addition, the hardness of the specimen increases with the increase of the ausforming strain amount, whereas the ausforming temperature has little effect on the hardness.

Disciplines

Engineering | Science and Technology Studies

Publication Details

Tian, J., Chen, G., Xu, Y., Jiang, Z. & Xu, G. (2019). Comprehensive Analysis of the Effect of Ausforming on the Martensite Start Temperature in a Fe-C-Mn-Si Medium-Carbon High-Strength Bainite Steel. *Metallurgical and Materials Transactions A: Physical Metallurgy and Materials Science*, 50 (10), 4541-4549.

1 **Comprehensive analysis of the effect of ausforming on martensite start**
2 **temperature in a Fe-C-Mn-Si medium-carbon high-strength bainite steel**

3 Junyu Tian^a, Guanghui Chen^a, Yaowen Xu^{a,*}, Zhengyi Jiang^b, Guang Xu^{a,*}

4 ^{a)} *The State Key Laboratory of Refractories and Metallurgy, Wuhan University of*
5 *Science and Technology, Wuhan 430081, China;*

6 ^{b)} *School of Mechanical, Materials, Mechatronic and Biomedical Engineering,*
7 *University of Wollongong, Wollongong, NSW 2522 Australia.*

8 Junyu Tian, E-mail: 13164178028@163.com; Guanghui Chen, E-mail:

9 chengguanghui@wust.edu.cn; *Corresponding author: Yaowen Xu, E-mail:

10 xuyw@wust.edu.cn; Zhengyi Jiang, E-mail: jiang@uow.edu.au; *Corresponding

11 author: Guang Xu, E-mail: xuguang@wust.edu.cn.

12 **Abstract:** The comprehensive effect of strain and ausforming temperature on the
13 martensite start temperature (M_S) of a medium-carbon bainite steel was investigated
14 by thermal simulation, optical microscope (OM), scanning electron microscope (SEM)
15 etc. It is already known that small strain increases the M_S , while larger strain
16 decreases M_S . But, the effect of ausforming temperature on M_S has not been reported
17 and clarified. In this study, the concepts of critical strain (ϵ_c) and saturated strain (ϵ_s)
18 are proposed. The M_S at the critical strain is equal to the M_S of the non-deformed
19 specimen. The saturation strain, which is first observed, is the strain value, and the M_S
20 at which does not further decrease with the increasing strain. The results show that the
21 temperature of M_S depends on the strain amount of ausforming, but is not affected by
22 the ausforming temperature. Moreover, with the increase of strain amount and
23 ausforming temperature, the length of the martensite laths decreases. In addition, the
24 hardness of specimen increases with the increase of ausforming strain amount,
25 whereas the ausforming temperature has little effect on the hardness.

26 **Keywords:** ausforming; martensite start temperature; critical strain; saturation strain;
27 microstructure; hardness

28

1 **1 Introduction**

2 The strength of steels is one of the main indexes in developing the new generation
3 steels. Bainite steel with better mechanical properties is one of the advanced high
4 strength steels [1-4]. Bhadeshia and Caballero proposed a novel nano-structured
5 superbainite steel with an ultimate tensile strength of 2.5 GPa [5-7]. A very low
6 transformation temperature near the martensite start temperature (M_S) is necessary to
7 obtain the nano-structured bainite plates. In addition, ausforming is an indispensable
8 step in the production of metals. It has been proved that ausforming affects the M_S .
9 Therefore, the investigation on the effect of ausforming on the M_S is significant for
10 the control of the transformation and microstructure of the superbainite steel.

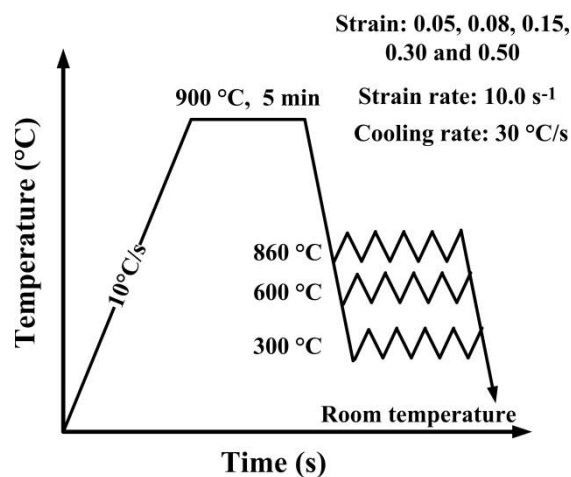
11 It is generally acknowledged that the deformation causes the mechanical
12 stabilization of austenite, i.e. M_S decreases after deformation [8-14]. For example, the
13 effect of ausforming on martensite transformation and microstructure in a
14 medium-carbon Si-Al-rich alloy was investigated by Zhang et al. [8,9]. They found
15 that ausforming decreased the M_S due to resisting of γ - α interface motion by
16 dislocation debris. The similar results were reported in Refs. [10-14]. However, a
17 different result was proposed by He et al. [15]. They studied the effect of ausforming
18 amount on the M_S in a 0.22 C (wt.%) low-carbon steel and claimed that a small
19 deformation increases the M_S , while a large deformation decreases the M_S
20 temperature. Summarizing the results of existing references, it is known that
21 ausforming strain amount has various effects on the M_S , so it is significant to further
22 study the effects of ausforming strain amount on M_S .

1 More important, so far, the effects of the ausforming temperature and carbon
2 content on the M_S have not been reported and clarified. Therefore, the studies on the
3 effect of ausforming temperature and carbon content on the M_S are necessary. In the
4 present study, three different ausforming temperatures with different strain amounts
5 were designed to investigate the effects of the ausforming temperature, strain amount
6 and carbon content on the temperature of M_S . The work is meaningful for the control
7 of the transformation, microstructure and mechanical properties in nano-structured
8 bainite steels.

9 **2 Materials and methods**

10 The experimental steel is a Fe-0.40C-2.21Mn-1.54Si-0.22Mo (wt.%)
11 high-strength bainite steel. The steel was refined and cast in the form of 50 kg ingot
12 using a laboratory-scale vacuum furnace, followed by hot-rolling and air-cooling to
13 room temperature. And then the experimental steel was tempered at 700 °C for 24 h to
14 minimize interior stress and facilitate machining. The specimens for the thermal
15 simulation experiments were machined to cylinders of 6 mm diameter and 15 mm
16 height. The thermal simulation experiments were conducted on a Gleeble-3500
17 simulator. The specimens were heated to 900 °C at 10 °C s⁻¹ and isothermally held for
18 5 min for austenitization. And then, the austenitization specimens were respectively
19 quenched to 860, 600 and 300 °C at a high cooling rate. The cooling rate was fast
20 enough to avoid the high temperature transformation. Subsequently, the specimens
21 were compressed to strains of 5 %, 8 %, 15 %, 30 % and 50 % at a strain rate of 10 s⁻¹,
22 respectively. Finally, all deformed specimens were quenched to ambient temperature.

1 The specific experimental procedures were shown in Fig. 1. Besides, a specimen
2 without deformation was directly quenched to ambient temperature after austenization
3 at 900 °C to measure the M_S of non-deformed specimen. After thermal simulation
4 experiments, all specimens were mechanically polished and etched with 4% nital. The
5 microstructure was observed using a Zeiss optical microscope (OM) and a Nova 400
6 Nano scanning electron microscope (SEM). The hardness was measured using a
7 Vickers hardness tester.



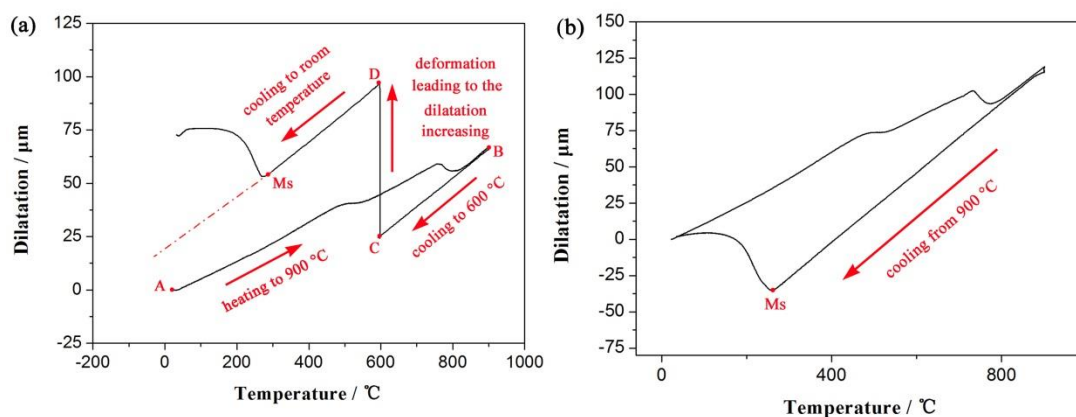
8
9 **Fig. 1** Experimental procedure

10 **3 Results and discussion**

11 *3.1 Analysis on the dilation*

12 Figure 2a presents an example (5 % strain deformation at 600 °C) to illustrate the
13 diameter change of specimen with temperature during the whole thermal simulation
14 process. The specimen was heated from ambient temperature to 900 °C for
15 austenization, resulting in the dilatation increasing (from point A to B). Then, the
16 specimen was cooled to 600 °C, resulting in the decrease in dilatation continuously
17 (from point B to C). After that, the specimen was compressed to 5% strain at 600 °C,

1 causing the vertical increase in dilatation (from point C to D). At last, the deformed
 2 specimen was cooled to ambient temperature and the dilatation decreased first and
 3 then increased. The inflection point represented the beginning of martensite
 4 transformation and corresponding temperature (M_S) was measured according to the
 5 tangent method [16].



6
 7 **Fig. 2** Example of dilatation change with temperature during the whole process: (a)
 8 600 °C+0.05 strain specimen; and (b) non-deformation specimen

9 As is widely known, high temperature diffusive transformation such as ferrite
 10 and bainite transformation is accompanied with the rejection of carbon atoms into
 11 surrounding untransformed austenite, resulting in the increase of the chemical
 12 stability of untransformed austenite [17-19], and thereby decreases the M_S . In addition,
 13 ausforming also affects ferrite and bainite transformation by providing heterogeneous
 14 nucleation [20-22], which may shorten the incubation time of transformation.
 15 Moreover, transformation may happen during deformation as well. To eliminate the
 16 influence caused by ferrite and bainite transformation on M_S , the cooling rate should
 17 be high enough to avoid ferrite and bainite transformation. Figure 2b shows the
 18 temperature-dilatation curves of specimen without deformation. The dilatation went

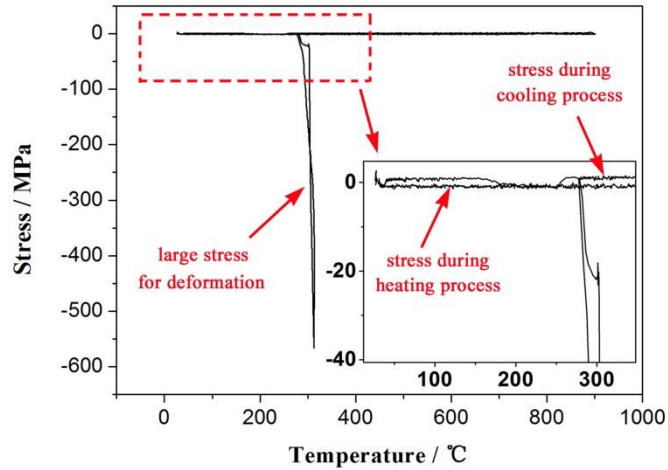
1 down straightly, indicating that no transformation happened before M_S . The dilatation
2 for deformed specimen (Fig. 2a) also went down straightly after deformation.
3 Therefore, the cooling rate in the present study was high enough to avoid high
4 temperature transformation.

5 For the deformation process, the deformation time can be calculated using
6 following Equation (1):

$$7 \quad -\ln(L/L_0) = \dot{\epsilon} \cdot t \quad (1)$$

8 where L and L_0 is the height of specimen after and before deformation, respectively.
9 The $\dot{\epsilon}$ is the strain rate ($\dot{\epsilon}=10 \text{ s}^{-1}$), and t is the consuming time for deformation. The
10 calculated time is 0.068 s for 0.05 strain. According to author's previous study [23],
11 there was no transformation during deformation.

12 In addition, it has been proved that stress influences the M_S as well [24, 25]. The
13 applied stress on the specimen for deformation was immediately unloaded after
14 deformation. Figure 3 shows the stress during the whole simulation experiment for
15 specimen with 15 % strain at 300 °C, illustrating that there was little stress during the
16 cooling process after deformation. This means that the M_S was not affected by stress.
17 Hence, it can be concluded that the changes of M_S in the present study were only
18 affected by ausforming, rather than other factors such as transformation and stress
19 before or during martensite transformation.

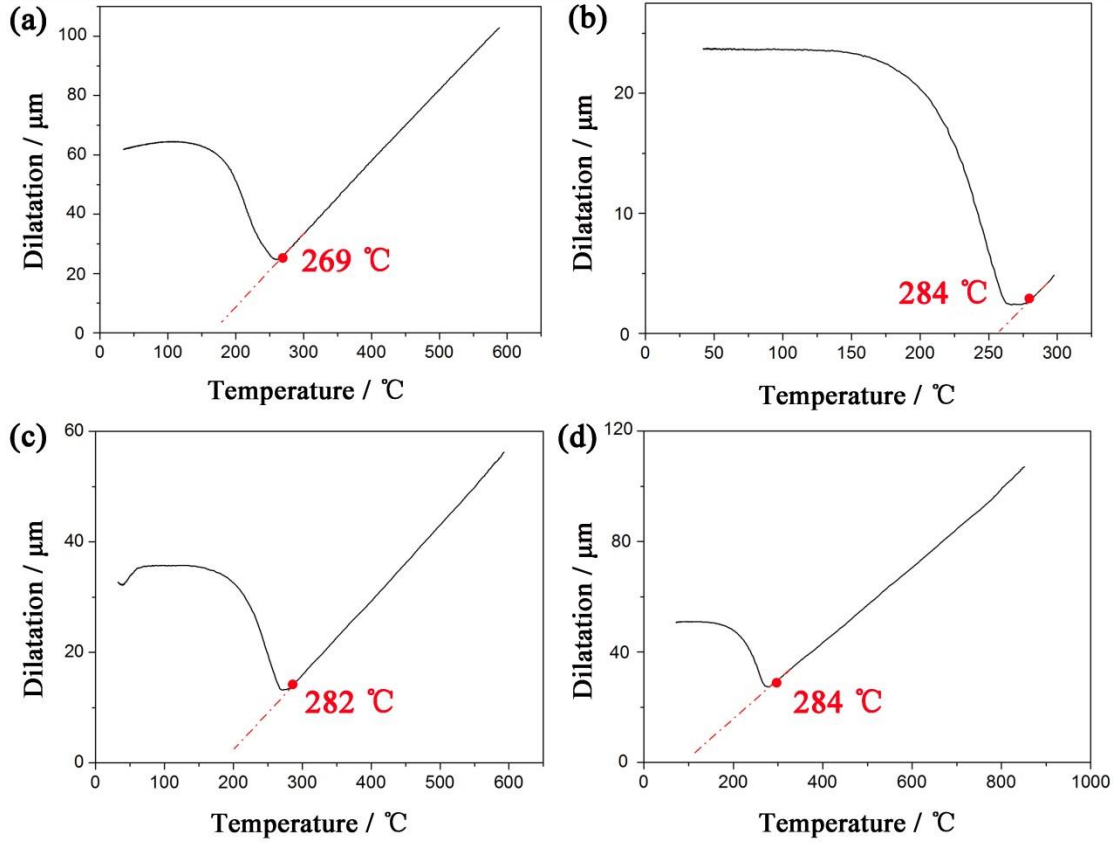


1

2 **Fig. 3** The change of stress during the whole simulation test for specimen with 0.15
 3 strain at 300 °C, illustrating the little influence of stress on M_S during cooling process

4 *3.2 Critical strain and saturation strain*

5 The M_S were determined based on the temperature-dilatation curves. Figure 4
 6 presents the curve of temperature and dilatation during cooling process of specimens
 7 without deformation and deformed to 0.05 strain at 300, 600 and 860 °C, respectively.
 8 During the cooling process, the undercooled austenite started to transform into
 9 martensite when the temperature reached M_S , resulting in obviously increase in
 10 dilatation. The M_S for specimen without deformation was 269 °C and M_S for
 11 specimens with 0.05 strain at different ausforming temperatures were 284, 282 and
 12 284 °C, respectively. Thus, compared with non-deformation, the ausforming with 0.05
 13 strain at different temperatures caused the increase of M_S .

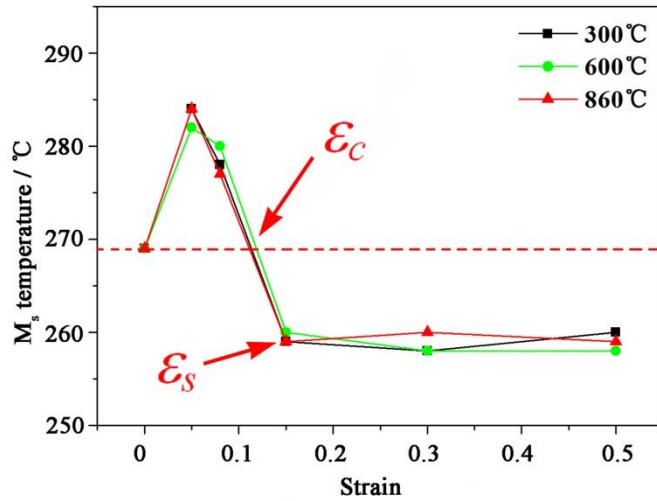


1

2 **Fig. 4** Temperature-dilatation curves illustrating the M_S of different specimens: (a)
 3 without deformation; (b) 300 °C+0.05 strain; (c) 600 °C+0.05 strain; and (d)
 4 860 °C+0.05 strain

5 The M_S for other deformed specimens were obtained using the same method and
 6 given in Fig. 5. It is clear that compared with the specimen without deformation, the
 7 M_S of deformed specimens first increased with strain, and then reached the peak value
 8 at the strain of 0.05. As the strain further increased, the M_S decreased. There was a
 9 critical strain (ε_c) between 0.05 and 0.15 strain, which was the inflection point of the
 10 effect of ausforming on the M_S . Compared with the M_S of non-deformed specimen,
 11 the ausforming increases the M_S temperature before reaching to ε_c , while it decreases
 12 the M_S after ε_c . In addition, the M_S reached a stable value at strain of 0.15, indicating
 13 that the increase of strain amount after 0.15 strain had no significant influence on the

1 M_S . The strain amount corresponding to the stable M_S is termed as saturation strain
2 (ϵ_s).



3

4 **Fig. 5** The change of M_S with strain amount and ausforming temperature

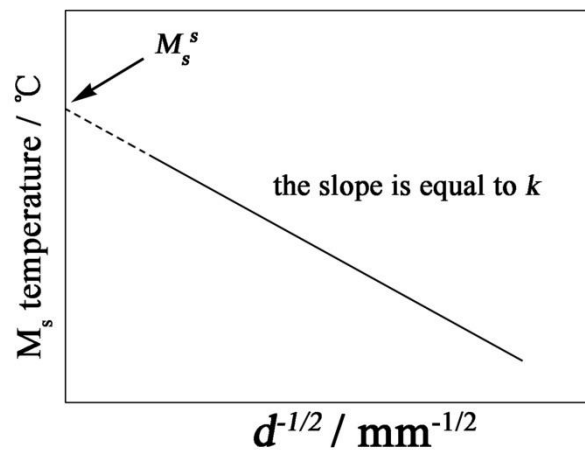
5 Figure 5 illustrates the effects of strain amount and ausforming temperature on
6 the M_S , indicating that the M_S did not change with ausforming temperature but was
7 distinctly affected by the deformation amount. The M_S firstly increased with the
8 increasing strain, and then reached the peak value when the strain amount was 0.05.
9 As the strain amount increased sequentially to 0.15, the M_S decreased sharply and was
10 apparently smaller than the M_S of specimen without deformation. The further increase
11 in deformation amount after 0.15 strain had no significant effect on the M_S , i.e. the M_S
12 tended to be constant. No matter at which temperature the specimen was deformed,
13 the M_S of specimen deformed for 0.05 strain was higher than that of non-deformed
14 specimen. The M_S of specimen with 0.15 strain was lower than that of non-deformed
15 specimen. This manifests that there must be a critical deformation amount ϵ_c (shown
16 in Fig. 5). The M_S increased by a small strain less than ϵ_c and decreased at a strain
17 larger than ϵ_c .

1 The M_S is affected by the size of austenite grains according to the Hall-Petch
2 formula (2) [26]:

$$3 \quad M_S = M_S^s - kd^{-1/2} \quad (2)$$

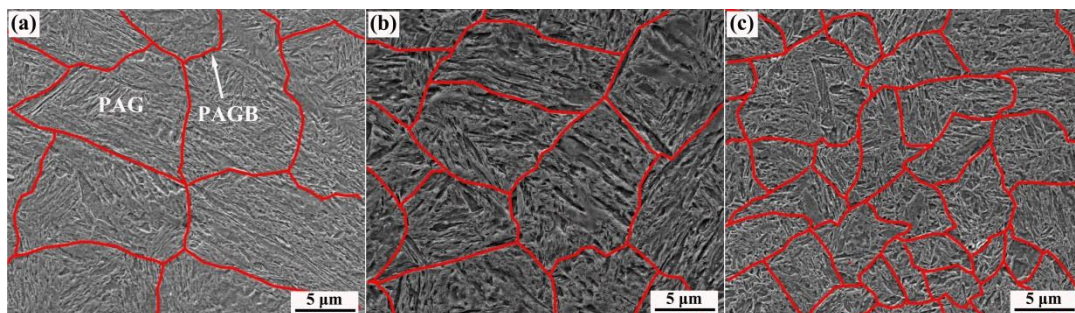
4 where the M_S is the martensite start temperature of polycrystalline material, and the
5 M_S^s is the martensite start temperature of single crystal material, of which the
6 diameter is regarded as infinity. The k is constant and the d is diameter of parent phase
7 grain (undercooled austenite). Therefore, the function of M_S and $d^{-1/2}$ is linear as
8 shown in Fig. 6, indicating that the M_S should increase with the diameter of the parent
9 phase grain. Figures 7a–c displays the micrographs of prior austenite grains (PAG)
10 and prior austenite grain boundaries (PAGB) of samples with different strains at
11 860 °C. The values of PAG were calculated by Image-Pro Plus software based on the
12 diagonal method. Two diagonals are drawn randomly in each grain. The average value
13 of the two diagonals is calculated as the size of this grain. Finally, the average value
14 of the sizes of all grains is selected as the grain size of the whole micrograph. In order
15 to achieve the higher accuracy, at least the results of three micrographs are reported
16 for each sample. The average sizes of PAG for samples deformed at 860 °C with 0.05,
17 0.15 and 0.50 strain were measured as 13.4 ± 2.3 , 10.3 ± 1.7 , and 6.2 ± 1.5 μm ,
18 respectively. Similarly, the PAG size of other samples deformed at 360 °C and 600 °C
19 with different strain amounts was also measured. The results are shown in Table 1. It
20 is obvious that the size of deformed austenite grains decreases with increasing strain.
21 In this study, however, the M_S increased with the strain when the deformation amount
22 was small. Then, the M_S decreased and tended to be constant as the strain increased

1 further. Hence, the M_s not only depended on the size of austenite grains, but also was
 2 affected by ausforming. In addition, the length of martensite laths is related to prior
 3 austenite grain size. The smaller austenite grain size results in shorter length of
 4 martensite laths. Hence, when the strain is large, the length of martensite laths is
 5 shorter (Fig. 11) due to smaller austenite grains. Although the length of martensite
 6 laths decreases with the increase of strain, the M_s temperature is not changed with the
 7 same trend, indicating that the length of martensite laths depends on not only the M_s
 8 temperature, but also, more importantly, strain amount.



9

10 **Fig. 6** The relationship between M_s and $d^{-1/2}$ according to Hall-Petch formula



11

12 **Fig. 7** Examples of PAG for samples deformed at 860 °C with different strains: (a)

13

0.05; (b) 0.15; and (c) 0.50

14

Table 1 The measured PAG of different deformed samples

Deformation temperature	Strain amount		
	0.05	0.15	0.50
300 °C	24.2±3.1	17.6±2.5	11.6±1.4
600 °C	18.4±1.8	13.1±1.4	9.5±1.7
860 °C	13.4±2.3	10.3±1.7	6.2±1.5

The displacive mechanism of martensitic transformation is generally accepted [27-29]. The formation of martensite consists of nucleation and growth. In a deformed austenite grain, the deformation leads to the formation of geometrically necessary dislocations (GNDs) at the austenite grain boundaries and randomly distributed dislocations within the austenite grains [30,31]. As the strain increases, the average of the density of GNDs increases linearly and the GNDs accumulate near the austenite grain boundaries. For the specimens with small strain, martensite transformation preferentially nucleates at the dislocations accumulated at the austenite grain boundaries before the formation of martensite. Once the primary martensite nucleates at the dislocations, the defect generated in the α - γ interfaces may immediately trigger further martensitic transformation in an autocatalytic chain-like manner. The small strain offers the preferential nucleation sites for martensitic transformation compared with the specimen without deformation. As a result, the M_S increases with strain smaller than the critical strain. The similar results were reported in Refs. [32-34].

With the further increasing strain (Fig. 5), however, the M_S decreased and then tended to be constant. When the strain was 0.08, the M_S was lower than that at 0.05 strain but still higher than that of non-deformed specimen. Besides, as the strain increased to the critical deformation amount ε_c , the M_S further decreased to be equal the M_S of non-deformed specimen. When the strain was larger than ε_c , the M_S of

1 deformed specimen was lower than that of non-deformed specimen and decreased
2 with the increasing strain until saturation strain (ε_s). Regarding to the deformed
3 specimens, the competitive relationship between nucleation and growth affects the
4 martensitic transformation and M_S . As the strain increases, the increasing amount of
5 dislocations remains inside the deformed austenite grains and leads to a high density
6 of dislocations, both which restricts the growth of martensite laths. Furthermore, the
7 appearance of subgrains induced by large strain also retards the growth of martensite
8 laths. Therefore, the martensite transformation was delayed and the M_S decreased.

9 When the strain increased from 0.15 to 0.50, the M_S tended to be constant. The
10 restricting effect of deformation on the M_S was saturated when the strain was 0.15. In
11 Kundu's research [31], the dislocations introduced by large strain also accumulate at
12 the boundaries of subgrains, thus providing nucleation sites for martensitic
13 transformation at a later stage. The martensite laths forming at the boundaries of
14 subgrains rapidly grow and stop at the other side of the subgrain boundaries. The
15 dislocations accumulated at the subgrain boundaries are saturated when the strain is
16 large enough [15]. Hence, the extent to which the saturated dislocations promote
17 nucleation does not change with increasing strain, resulting in basically stable M_S .

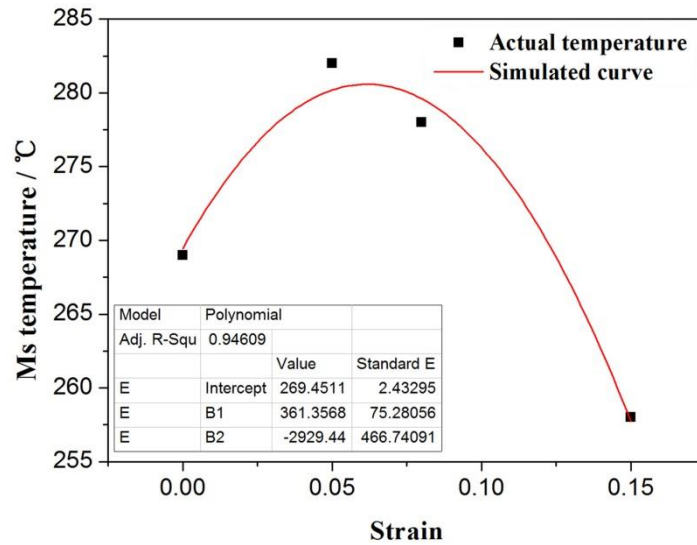
18 In previous study, the effect of ausforming strain amount on the M_S in a
19 low-carbon bainite steel was studied by He et al. [15]. They claimed that the small
20 strain increases the M_S while large strain decreases the M_S . The similar result was
21 obtained in a medium-carbon bainite steel in the present research. However, in their
22 study, the critical strain amount ε_c was about 0.23 for a low-carbon steel, while it was

1 about 0.10 for a medium-carbon steel in this study. This means that the critical strain
2 depends on the chemical composition of steel, especially carbon content. Moreover,
3 the saturated strain ε_s was not observed and defined in previous study, whereas it was
4 firstly observed and defined in the present study. Compared with low-carbon steels,
5 medium-carbon steels contain more carbon and other alloying element such as
6 manganese (Mn) and silicon (Si), resulting in more elastic distortion. On the other
7 hand, the solute atoms segregated on the dislocations have the pinning effect on the
8 dislocations. Thus, more serious work hardening happens in medium-carbon steels,
9 causing the decrease of ε_c . In addition, summarizing the experimental results of the
10 two kinds of steels, it can be inferred that although the appeared in medium-carbon
11 steel but not in low-carbon steels, the ε_s may still appear in low-carbon steel when a
12 certain very large strain was loaded.

13 The regression equation reflecting the influence of strain amount on M_S is given
14 as following Equation (3) using the software of Origin 8.0:

$$15 \quad M_S = 269.4511 + 361.3568\varepsilon - 2929.44\varepsilon^2 \quad (3)$$

16 where the ε is the strain amount, indicating that the M_S follows the parabola law
17 before the ε_s . Figure 8 presents the measured value and the corresponding simulated
18 curve ($\varepsilon < 0.15$). The correlation coefficient is 0.94609, meaning that the Equation (3)
19 is of good precision.

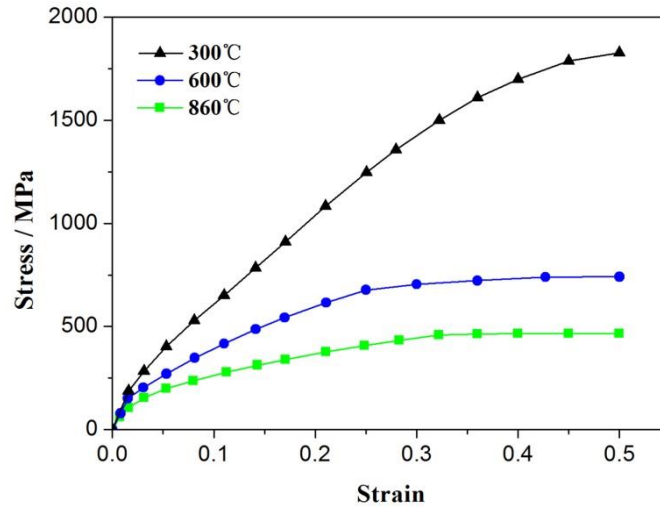


1

2 **Fig. 8** M_S change following the parabola law at the strain before reaching the ϵ_s

3 *3.3 Effect of ausforming temperature on M_S*

4 It is observed in Fig. 5 that different ausforming temperatures (300, 600 and
5 860 °C) had no significant effect on M_S , critical strain ϵ_c and saturated strain ϵ_s . The
6 stress-strain curves during the compression deformation process at different
7 ausforming temperatures are presented in Fig. 9. It indicates that no dynamic
8 recrystallization occurred for all deformation conditions. Obvious dynamic recovery
9 happened at 600 and 860 °C, while little dynamic recovery occurred at 300 °C.
10 Theoretically, the density of the dislocations near austenite grain boundaries in the
11 specimens deformed at 300 °C should be higher than that in other two specimens with
12 deformation at 600 and 860 °C. It should have led to the different M_S in different
13 specimens at different ausforming temperatures. However, according to the results in
14 Fig. 5 the ausforming temperature has little effect on M_S . It implied that the influence
15 of austenite grain size cannot be ignored.



1

2 **Fig. 9** Stress-strain curves of the specimens deformed at 300, 600 and 860 °C,

3 indicating no dynamic recrystallization happened

4 The OM microstructures at different deformation conditions are shown in Fig. 10.

5 It illustrates that the size of austenite grains at 860 °C (Figs. 10e and 10f) was

6 apparently smaller than that at 300 °C (Figs. 10a and 10b). For the specimens

7 deformed at different temperatures, the higher ausforming temperature caused the

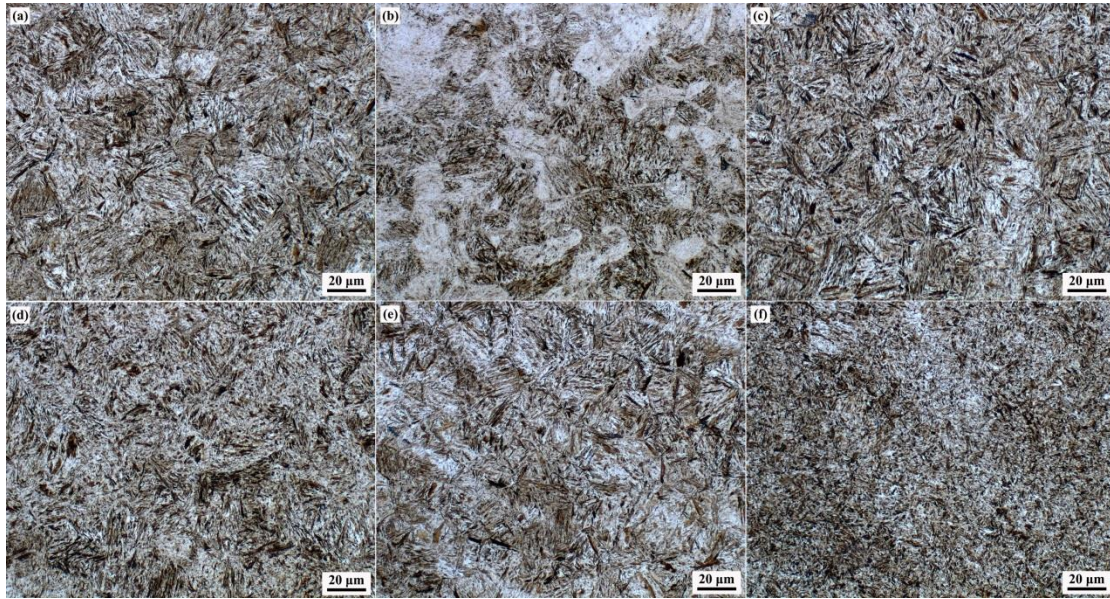
8 smaller density of dislocations, leading to the decrease of M_s . But smaller grain size

9 at high ausforming temperature provided more nucleation sites for martensite

10 transformation. It is the combination of the dislocation density and austenite grain size

11 that affects the M_s , contributing to the little influence of ausforming temperature on

12 M_s . It is a main novelty in this study.



1

2

3

4

5

6

7

8

9

10

11

12

13

14

15

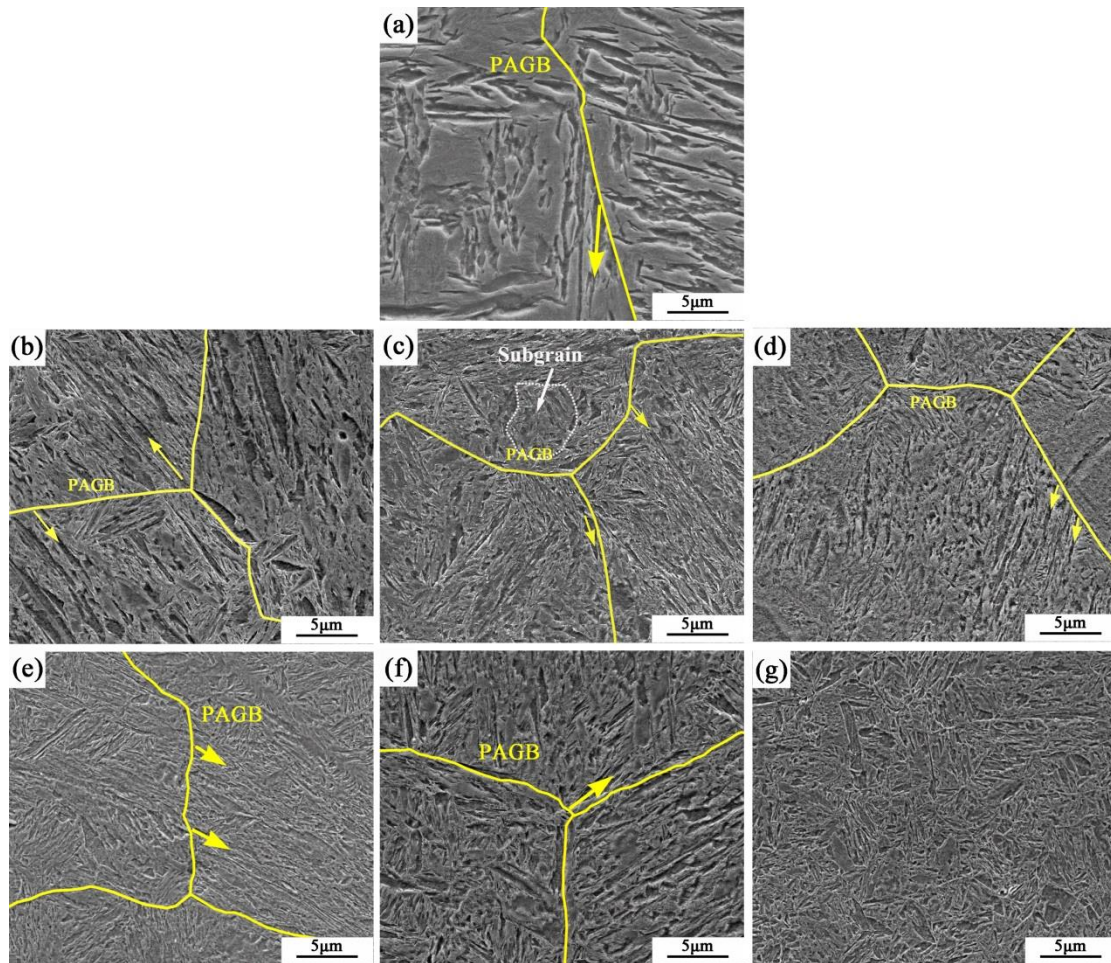
16

Fig. 10 The OM microstructure of different specimens: (a) 300 °C+0.05 strain; (b) 300 °C+0.50 strain; (c) 600 °C+0.05 strain; (d) 600 °C+0.50 strain; (e) 860 °C+0.05 strain; and (f) 860 °C+0.50 strain

3.4 Microstructure

The microstructure illustrates that the size of the austenite grains decreased with the increasing ausforming temperature (Fig. 10). The austenite grains tended to be broken by the deformation at a high temperature. For the specimens deformed at 860 °C, the austenite grains were the finest at the same strain amount, leading to the shortest martensite laths. The micrographs with a higher magnification of 10000x of the specimens treated by different ausforming conditions are presented in Fig. 11, indicating that the growth of martensite laths in original austenite is hindered by subgrain boundary (Fig. 11c). And the similar phenomenon was also observed in Ref. [15]. In addition, martensite laths grow from the prior austenite grain boundary (PAGB), as marked with arrow in Figs. 11a-e. It is difficult to observe the martensite laths on PAGB in Fig. 11f due to the finest microstructure. In addition, it also can be

1 observed that the martensite laths of non-deformed specimen (Fig. 11a) were longer
2 than those of deformed specimens. It can be observed that the length of martensite
3 laths decreased with the increasing strain (Figs. 11b-d and Figs. 11e-g). The growth of
4 martensite laths was limited in austenite grains. When the strain amount was small
5 ($\epsilon=0.05$), the prior austenite grains were larger, resulting in the longer martensite laths.
6 The prior austenite grains became smaller with the increase of strain, leading to the
7 shorter martensite laths (Figs. 11d and 11g). This is attributed to the growth
8 retardation of martensite by subgrain boundaries. For specimens with the largest strain
9 of 0.50, the parent austenite grains were obviously broken, resulting in the shortest
10 martensite laths. Moreover, compared with the specimens deformed at 300 °C, the
11 size of martensite laths at 860 °C was shorter. This is because austenite grains are
12 easily broken at high ausforming temperature.



1

2

3

4

5

6

7

8

9

10

11

12

Fig. 11 The SEM microstructure of specimens treated by different processes: (a)

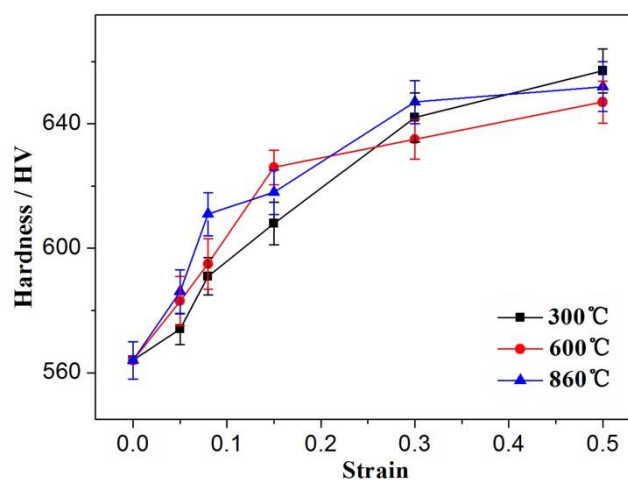
without deformation; (b) 300 °C+0.05 strain; (c) 300 °C+0.15 strain; (d) 300 °C+0.50

strain; (e) 860 °C+0.05 strain; (f) 860 °C+0.15 strain; and (g) 860 °C+0.50 strain

3.5 Effect of ausforming on the hardness

The hardnesses of different specimens were given in Fig. 12. It indicates that the work hardening caused the increase of hardness with strain amount, while the ausforming temperature had little effect on the hardness. When the ausforming temperature was same, the increasing strain led to the decrease in the austenite grain size and the increase in the dislocation density, contributing to the increase of hardness with strain. The change in hardness is related to the morphology of martensite laths. Smaller austenite grain hinders the growth of martensite laths. Hence, when the strain

1 amount is large, the martensite laths are refined (Fig. 11), resulting in a larger
2 hardness of the microstructure. Therefore, the hardness increased with strain. It is
3 noted that the ausforming temperature had no significant effect on the hardness,
4 which was consistent with the effect of ausforming temperature on the M_S . Therefore,
5 the hardness was mainly affected by the austenite grain size and the dislocation
6 density in this study, while the M_S had no obvious influence on it.



7
8 **Fig. 12** The Vicker's hardness of specimens

9 In the present study, the effect of ausforming deformation on M_S mainly focuses
10 on the compressive strain. The purpose of the present research is to provide
11 theoretical reference for industrial production. The deformation on austenite in
12 industrial production is normally compressive deformation. Therefore, tensile
13 deformation and hydrostatic stress was not studied here. The effect of tensile
14 deformation and hydrostatic stress on M_S should be conducted in the future study.

15 **4 Conclusions**

16 The effects of ausforming on the M_S in a Fe-C-Mn-Si medium-carbon bainite steel
17 were investigated. The following conclusions can be drawn:

1 (1) The saturation strain ε_s is firstly observed and defined. The M_S tends to be
2 constant when the strain is larger than ε_s . Moreover, the critical strain ε_c is proposed.
3 The strain smaller than ε_c increases the M_S , whereas the M_S decreases at the strain
4 larger than ε_c .

5 (2) The ausforming temperature does not affect the M_S . The critical strain ε_c and
6 saturation strain ε_s are not affected by the ausforming temperature.

7 (3) The length of martensite laths decreases with the increase of ausforming
8 temperature and strain amount.

9 (4) The hardness of specimens increases with strain amount, while it is not
10 affected by the ausforming temperature.

11 **Acknowledgements**

12 The authors gratefully acknowledge the financial supports from the National
13 Natural Science Foundation of China (Nos.51874216 and 51704217), the Major
14 Projects of Technology Innovation of Hubei Province (No.2017AAA116), the Science
15 and Technology Project of Wuhan (2018010402011187), Hebei Joint Research Fund
16 for Iron and Steel (E2018318013), Youth Foundation of Wuhan University of Science
17 and Technology (2015XZ002), the State Key Laboratory Science Foundation for
18 Youths (2016QN10) and the State Scholarship Fund of China Scholarship Council.

19 **References**

20 [1] H.J. Hu, G. Xu, L. Wang, Z.L. Xue, Y.L. Zhang and G.H. Liu: *Mater. Des.* 2015,
21 vol. 84, pp.95-99.

22 [2] Y.X. Zhou, X.T. Song, J.W. Liang, Y.F. Shen and R.D.K. Misra: *Mater. Sci. Eng. A*

- 1 2018, vol. 718, pp. 267-76.
- 2 [3] J. Zhao, K. Guo, Y.M. He, Y.F. Wnag and T.S. Wang: *Scripta Mater.* 2018, vol. 152,
3 pp. 20-23.
- 4 [4] G.H. Chen, G. Xu, H.S. Zurob, H.J. Hu and X.L. Wan: *Metall. Mater. Trans. A*
5 2019, vol. 50, pp. 573-80.
- 6 [5] C. García-mateo, F.G. Caballero and H.K.D.H. Bhadeshia: *Mater. Sci. Forum*
7 2015, vol. 112, pp. 285-88.
- 8 [6] F.G. Caballero, C. García-mateo and M.K. Miller: *JOM* 2014, vol. 66, pp. 747-55.
- 9 [7] F.G. Caballero, C. García-mateo, C. Capdevila and C. García de Andrés: *Mater.*
10 *Manuf. Process.* 2007, vol. 22, pp. 502-06.
- 11 [8] M. Maalekian, E. Kozeschnik, S. Chatterjee and H.K.D.H. Bhadeshia: *Met. Sci. J.*
12 2007, vol. 23, pp. 610-12.
- 13 [9] S. Chatterjee, H.S. Wang, J.R. Yang and H.K.D.H. Bhadeshia: *Met. Sci. Technol.*
14 2006, vol. 22, 641-44.
- 15 [10] J.R. Strife, M.J. Carr and G.S. Ansell: *Metall. Trans. A* 1976, vol. 8, 1471-84.
- 16 [11] M. Zhang, Y.H. Wang, C.L. Zheng, F.Z. Zhang and T.S. Wang: *Mater. Des.* 2014,
17 vol. 62, pp. 168-74.
- 18 [12] M. Zhang, Y.H. Wang, C.L. Zheng, F.Z. Zhang and T.S. Wang: *Mater. Sci. Eng. A*
19 2014, vol. 596, 9-14.
- 20 [13] T. Sadasue, S. Suzuki, M. Suwa, S. Mitao and K. Takahashi: *Mater. Sci. Forum*
21 2003, vol. 426, 1493-98.
- 22 [14] T.S. Wang, M. Zhang, Y.H. Wang, J. Yang and F.C. Zhang: *Scripta Mater.* 2013,

- 1 vol. 68, 162-65.
- 2 [15] B.B. He, W. Xu and M.X. Huang: *Mater. Sci. Eng. A* 2014, vol. 609, 141-46.
- 3 [16] Y.C. Liu, D.J. Wang, F. Sommer and E.J. Mittemeijer: *Acta Mater.* 2008, vol. 56,
4 3833-42.
- 5 [17] H.J. Hu, G. Xu, L. Wang, M.X. Zhou and Z.L. Xue: *Met. Mater. Int.* 2015, vol.
6 21, pp. 929-35.
- 7 [18] L.C. Chang and H.K.D.H. Bhadeshia: *Mater. Sci. Eng. A* 1994, vol. 184, pp.
8 17-19.
- 9 [19] G. Xu, H. Zou and C.H. Bu: *Adv. Mater. Res.* 2011, vol. 415, pp. 974-78.
- 10 [20] J.G. He, A.M. Zhao, C. Zhi and H.L. Fan: *Scripta Mater.* 2015, vol. 107, pp.
11 71-74.
- 12 [21] H.J. Hu, H.S. Zurob, G. Xu, D. Embury and G.R. Purdy: *Mater. Sci. Eng. A* 2015,
13 vol. 626, pp. 34-40.
- 14 [22] H.J. Hu, G. Xu, L. Wang and M.X. Zhou: *Steel Res. Int.* 2016,
15 DOI: 10.1002/srin.201600170.
- 16 [23] G.H. Chen, G. Xu, H.J. Hu, Q. Yuan and Q.X. Zhang: *Steel Res. Int.* 2018, DOI:
17 10.1002/srin.201800201.
- 18 [24] M.T. Todinov, J.F. Knott and M. Strangwood: *Acta Mater.* 1996, vol. 44,
19 4909-15.
- 20 [25] J.R. Patel and M. Cohen: *Acta Metall.* 1953, vol. 1, 531-38.
- 21 [26] J.X. Wu, B.H. Jiang and T.Y. Hsu: *Acta Metall. Sin.* 1988, vol. 36, 1521-26.
- 22 [27] Y. Tian, A. Borgenstam and P. Hedström: *J. Alloys Compd.* 2018, vol. 766, pp.

1 131-39.

2 [28] X.D. Zhang, J.Q. Ren and X.D. Ding: *Appl. Compos. Mater.* 2018, DOI:
3 10.1007/s10443-018-9701-5.

4 [29] M. Eskandari, M.A. Mohtadi-Bonab, A. Zarei-Hanzaki, A.G. Odeshi and J.A.
5 Szpunar: *J. Mater. Eng. Perform.* 2016, vol. 25, pp. 1611-20.

6 [30] M.F. Ashby: *Philos. Mag. A* 1970, vol. 21, pp. 399-24.

7 [31] A. Kundu and D.P. Field: *Metall. Mater. Trans. A* 2018, vol. 49, pp. 3274-82.

8 [32] T. Song and B.C.D. Cooman: *ISIJ Int.* 2014, vol. 54, pp. 2394-03.

9 [33] S. Dash and N. Brown: *Acta Metall.* 1966, vol. 14, pp. 595-03.

10 [34] L. Samek E.D. Moor, J. Penning, and B.C.D. Cooman: *Metall. Mater. Trans. A*
11 2006, vol. 37, pp. 109-124.

12

1 **Table captions**

2 **Table 1** The measured PAG of different deformed samples

Deformation temperature	Strain amount		
	0.05	0.15	0.50
300 °C	24.2±3.1	17.6±2.5	11.6±1.4
600 °C	18.4±1.8	13.1±1.4	9.5±1.7
860 °C	13.4±2.3	10.3±1.7	6.2±1.5

3

1 **Figures captions**

2 **Fig. 1** Experimental procedure

3 **Fig. 2** Example of dilatation change with temperature during the whole process: (a)
4 600 °C+0.05 strain specimen; and (b) non-deformation specimen

5 **Fig. 3** The change of stress during the whole simulation test for specimen with 0.15
6 strain at 300 °C, illustrating the little influence of stress on M_S during cooling process

7 **Fig. 4** Temperature-dilatation curves illustrating the M_S of different specimens: (a)
8 without deformation; (b) 300 °C+0.05 strain; (c) 600 °C+0.05 strain; and (d)
9 860 °C+0.05 strain

10 **Fig. 5** The change of M_S with strain amount and ausforming temperature

11 **Fig. 6** The relationship between M_S and $d^{-1/2}$ according to Hall-Petch formula

12 **Fig. 7** Examples of PAG for samples deformed at 860 °C with different strain amount:
13 (a) 0.05; (b) 0.15; and (c) 0.50

14 **Fig. 8** M_S change following the parabola law at the strain before reaching the ε_s

15 **Fig. 9** Stress-strain curves of the specimens deformed at 300, 600 and 860 °C,
16 indicating no dynamic recrystallization happened

17 **Fig. 10** The OM microstructure of different specimens: (a) 300 °C+0.05 strain; (b)
18 300 °C+0.50 strain; (c) 600 °C+0.05 strain; (d) 600 °C+0.50 strain; (e) 860 °C+0.05
19 strain; and (f) 860 °C+0.50 strain

20 **Fig. 11** The SEM microstructure of specimens treated by different processes: (a)
21 without deformation; (b) 300 °C+0.05 strain; (c) 300 °C+0.15 strain; (d) 300 °C+0.50
22 strain; (e) 860 °C+0.05 strain; (f) 860 °C+0.15 strain; and (g) 860 °C+0.50 strain

23 **Fig. 12** The Vicker's hardness of specimens